Development of Multi-Hierarchy Simulation Model with Non-Uniform Space Grids for Collisionless Driven Reconnection

Theoretical studies of molecular ions: Be 2

K. D. Jordan and Jack Simons

Citation: The Journal of Chemical Physics **65**, 1601 (1976); doi: 10.1063/1.433223
View online: http://dx.doi.org/10.1063/1.433223
View Table of Contents: http://scitation.aip.org/content/aip/journal/jcp/65/4?ver=pdfcov
Published by the AIP Publishing

Development of multi-hierarchy simulation model with non-uniform space grids for collisionless driven reconnection

Shunsuke Usami,[1,a)] Ritoku Horiuchi,[1,2] Hiroaki Ohtani,[1,2] and Mitsue Den[3]
[1]*Department of Helical Plasma Research, National Institute for Fusion Science, Toki 509-5292, Japan*
[2]*The Graduate University for Advanced Studies (Soken-dai), Toki 509-5292, Japan*
[3]*National Institute of Information and Communications Technology, Koganei 184-8795, Japan*

(Received 1 October 2012; accepted 18 December 2012; published online 18 June 2013)

A multi-hierarchy simulation model aimed at magnetic reconnection studies has been developed, in which macroscopic and microscopic physics are solved self-consistently and simultaneously. In this work, the previous multi-hierarchy model by these authors is extended to a more realistic one with non-uniform space grids. Based on the domain decomposition method, the multi-hierarchy model consists of three parts: a magnetohydrodynamics algorithm to express the macroscopic global dynamics, a particle-in-cell algorithm to describe the microscopic kinetic physics, and an interface algorithm to interlock macro and micro hierarchies. For its verification, plasma flow injection is simulated in this multi-hierarchy model and it is confirmed that the interlocking method can describe the correct physics. Furthermore, this model is applied to collisionless driven reconnection in an open system. Magnetic reconnection is found to occur in a micro hierarchy by injecting plasma from a macro hierarchy. © *2013 AIP Publishing LLC*.
[http://dx.doi.org/10.1063/1.4811121]

I. INTRODUCTION

Magnetic reconnection is a typical nonlinear complex phenomenon controlled by multiple spatiotemporal scale physics. Some microscopic processes generating electrical resistivity, for instance, wave-particle interaction,[1–4] are needed as a trigger of magnetic reconnection. On the other hand, field topology changes on a macroscopic scale and global plasma transport occurs as a result of magnetic reconnection. These macroscopic and microscopic physics phenomena are strongly and complexly coupled.

Two different types of simulation techniques, a fully kinetic electromagnetic particle-in-cell (PIC) simulation and a magnetohydrodynamics (MHD) simulation have been applied to investigate the magnetic reconnection process. MHD simulations[5,6] are widely used to investigate macroscopic behavior of magnetic reconnection phenomenologically. However, electrical resistivity is set artificially by introducing some assumptions in the MHD equations. Its generation mechanism cannot be described in the MHD framework. On the other hand, PIC simulations[3,4,7–11] have demonstrated the microscopic process of magnetic reconnection from the first principle, thus, the generation mechanism of electrical resistivity can be treated self-consistently. However, computer resources required for PIC simulations are too huge to execute large-scale and long-time simulations such as the entire geomagnetosphere.

In order to clarify the complete picture of magnetic reconnection as a multi-hierarchy phenomenon, we have developed a multi-hierarchy simulation model, which deals with both macroscopic and microscopic physics self-consistently and simultaneously. The developed multi-hierarchy model is applied to two test programs to examine its physical reliability. The first is propagation of linear Alfvén waves,[12,13] and the other one is plasma injection from a macro hierarchy to a micro hierarchy.[14] Then, we have further applied our model to magnetic reconnection in a simple multi-hierarchy system and have succeeded in the first demonstration of collisionless driven reconnection, in which plasma inflows come from a macro hierarchy to a micro hierarchy and drive magnetic reconnection in the micro hierarchy.[15,16]

In this paper, we discuss a recent improvement of our multi-hierarchy model aiming to apply it to more realistic systems. In Sec. II, we explain a model with non-uniform spatial grids as an improved version from previous multi-hierarchy models[12–16] and review the interlocking method between macro and micro hierarchies.[12,15] In Sec. III A, we perform multi-hierarchy simulations of plasma injection in order to examine the physical reliability of the interlocking method in the improved model. It is confirmed that plasmas flow smoothly and continuously. Finally, our improved model is applied to magnetic reconnection and the multi-hierarchy simulation results are compared with the pure PIC simulation results in Sec. III B. Section IV gives a summary of our work.

II. MULTI-HIERARCHY MODEL

A. Domain decomposition method with non-uniform space grids

Let us explain a hierarchical structure of magnetic reconnection in the upstream direction. The characteristic spatial and temporal scales differ by domain.[9] For reconnection with no guide field, in the vicinity of the reconnection point, a gyroradius is much larger than the typical spatial scale of the background plasma such as the width of a current sheet. As the guide field is stronger, charged particles become strongly magnetized, so inertia effect is expected to

[a)]Electronic address: usami.shunsuke@nifs.ac.jp

be significant.[10] Thus, a microscopic kinetic model is required to describe particle dynamics. On the other hand, as being away from the reconnection point, phenomena relax to large-scale and slow behavior. Therefore, a macroscopic one-fluid model can give a good approximation to express global dynamics.

Based on the feature described above, our multi-hierarchy model employs a domain decomposition method.[12–16] Figure 1 shows the schematic diagram of the multi-hierarchy model for magnetic reconnection. The simulation domain is divided into three domains, the MHD, PIC, and interface domains in the upstream direction along the y axis. The MHD and PIC domains are interlocked via the interface domain. In the MHD domain, the MHD simulation algorithm is used to describe global dynamics, since plasma dynamics in this domain is assumed to be expressed by the one-fluid model. On the other hand, the physics in the PIC domain is solved by the PIC simulation algorithm, since microscopic kinetic effects play important roles. The physics in the interface domain with a finite width is treated by both the MHD and PIC algorithms. In Sec. II B, an interlocking method in the interface domain is explained. The interface domain thus needs to be located far away from the reconnection point, where the MHD approximation is fully satisfied.

In previous works,[12–16] we have used uniform space grids in the whole domain of the multi-hierarchy model. In this work, we adopt non-uniform space grids in the y-axis along the upstream direction. The grid spacing Δy is given as a function of the space coordinate y, as shown in Fig. 2. The grid spacing in the PIC domain is a quarter of that at the boundary layer of the MHD domains. In the region between $y = -y_c$ and $y = y_c$ which covers the PIC domain, the interface domain, and the MHD domain in the vicinity of the interface domain, Δy is taken to be a constant minimum value. On the other hand, the grid spacing Δx and Δz remain constant, which are equal to those in the PIC domain.

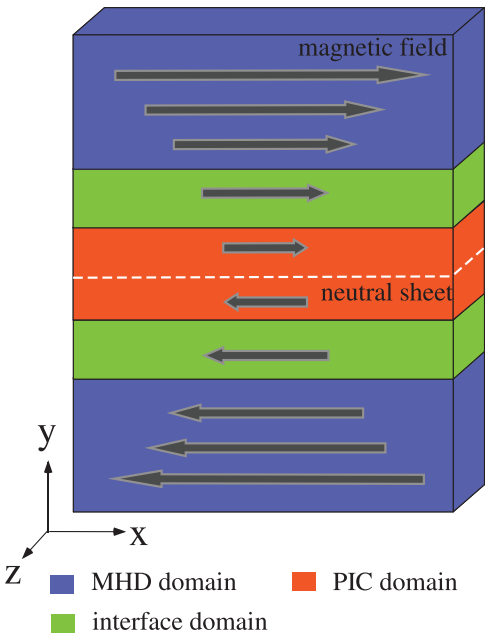

FIG. 1. Schematic diagram of the multi-hierarchy simulation box for magnetic reconnection studies. The simulation domain is divided into PIC, interface, and MHD domains.

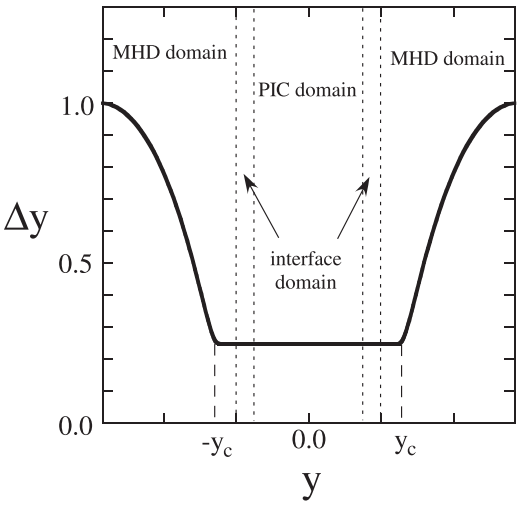

FIG. 2. Grid spacing Δy vs space coordinate y. In the MHD domain, Δy is non-uniform.

B. Overview of interlocking method

The data of the PIC and MHD algorithms are interconnected in the same manner as in previous models, as shown in Refs. 12–16. We, however, outline the interlocking method between the PIC and MHD domains in this subsection.

In the MHD algorithm, the following basic equations are solved:

$$\frac{\partial \rho}{\partial t} = -\nabla \cdot (\rho \boldsymbol{u}), \tag{1}$$

$$\frac{\partial (\rho \boldsymbol{u})}{\partial t} = -\nabla \cdot (\rho \boldsymbol{u}\boldsymbol{u}) - \nabla P + \frac{1}{4\pi}(\nabla \times \boldsymbol{B}) \times \boldsymbol{B}, \tag{2}$$

$$\frac{\partial \boldsymbol{B}}{\partial t} = \nabla \times (\boldsymbol{u} \times \boldsymbol{B}), \tag{3}$$

$$\frac{\partial P}{\partial t} = -\nabla \cdot (P\boldsymbol{u}) - (\Gamma - 1)P\nabla \cdot \boldsymbol{u}, \tag{4}$$

where ρ, $\boldsymbol{u}$, $\boldsymbol{B}$, P, and Γ denote the mass density, fluid velocity, magnetic field, pressure, and ratio of specific heats, respectively. On the other hand, the governing equations in the PIC algorithm[17] are

$$\frac{1}{c}\frac{\partial \boldsymbol{B}}{\partial t} = -\nabla \times \boldsymbol{E}, \tag{5}$$

$$\frac{1}{c}\frac{\partial \boldsymbol{E}}{\partial t} = \nabla \times \boldsymbol{B} - \frac{4\pi}{c}\boldsymbol{J}, \tag{6}$$

$$\nabla \cdot \boldsymbol{B} = 0, \tag{7}$$

$$\nabla \cdot \boldsymbol{E} = 4\pi\rho_q, \tag{8}$$

$$\frac{d(\gamma_k \boldsymbol{v}_k)}{dt} = \frac{q_k}{m_k}\left(\boldsymbol{E} + \frac{\boldsymbol{v}_k}{c} \times \boldsymbol{B}\right), \tag{9}$$

$$\frac{d\boldsymbol{x}_k}{dt} = \boldsymbol{v}_k, \tag{10}$$

$$\boldsymbol{J} = \sum_{k=1}^{N} q_k \boldsymbol{v}_k S(\boldsymbol{x} - \boldsymbol{x}_k), \tag{11}$$

$$\rho_q = \sum_{k=1}^{N} q_k S(\boldsymbol{x} - \boldsymbol{x}_k). \tag{12}$$

Here $\boldsymbol{x}_k$, $\boldsymbol{v}_k$, m_k, q_k, and γ_k are the position, velocity, mass, charge, and Lorentz factor of the k-th particle, respectively, and $\boldsymbol{E}$, $\boldsymbol{J}$, and ρ_q denote the electric field, current density, and charge density, respectively. Also, N is the total number of particles and S is a form function of super-particles.[17]

First, let us discuss an interlocking scheme for macroscopic quantities such as fluid velocities and mass density. A macroscopic quantity in the interface domain, $Q_{\text{interface}}$, is given by the following interpolation relation:

$$Q_{\text{interface}} = FQ_{\text{MHD}} + (1 - F)Q_{\text{PIC}}. \tag{13}$$

We call this method the hand-shake scheme.[12,14,18] Here, Q_{MHD} is a macroscopic quantity calculated only by the MHD basic equations (1)–(4) and Q_{PIC} is a macroscopic quantity obtained only by the PIC governing equations (5)–(12). In the PIC algorithm, macroscopic quantities are obtained by assembling particle velocities and positions statistically. The interconnection function, F, generally depends on the coordinates (x, y, z). In this paper, hierarchy-interlocking is one-dimensional, so then F is given as a function of y

$$F(y) = \frac{1}{2}\left[1 + \cos\left(\pi \frac{y - y_{\text{MHD}}}{y_{\text{PIC}} - y_{\text{MHD}}}\right)\right], \tag{14}$$

where y_{MHD} and y_{PIC} are the boundary positions of the interface domain on the MHD and PIC sides, respectively. However, a different function

$$F(y) = \begin{cases} 1 & (\text{for } y \neq y_{\text{PIC}}) \\ 0 & (\text{for } y = y_{\text{PIC}}) \end{cases} \tag{15}$$

is used only for thermal velocity (pressure).[14] We discuss why a different function needs to be used for thermal velocity in Appendix A.

On the other hand, microscopic quantities such as positions and velocities of individual particles are needed in order to advance the PIC algorithm in the interface domain. It is assumed that the shifted Maxwellian velocity distribution is fully satisfied in the interface domain. In other words, we put the interface domain at the location where the shifted Maxwellian velocity distribution holds. At every PIC time step, all particles in the interface domain are removed and freshly loaded with particle velocities and positions determined so as to satisfy the profiles with the fluid velocity, $\boldsymbol{u}_{\text{interface}}$, number density, $n_{\text{interface}}$, and thermal velocity, $v_{T,\text{interface}}$. In order to generate the current density, $\boldsymbol{J}_{\text{interface}}$, electron particle velocities are given so that their averaged velocity is equal to $\boldsymbol{u}_{\text{interface}} - \boldsymbol{J}_{\text{interface}}/n_{\text{interface}}$.

Let us summarize the interlocking method between MHD and PIC data. In both MHD and PIC simulations, physical quantities at the next step, $n + 1$, can be expressed as a function of ones at the current time step n

$$(Q^{(n+1)}, q^{(n+1)}) = G(Q^{(n)}, q^{(n)}). \tag{16}$$

Here, $Q^{(n)}$ and $q^{(n)}$ are macroscopic and microscopic physical quantities, respectively, the superscript n represents the time step, and G corresponds to Eqs. (1)–(4) or Eqs. (5)–(12) and is a function of known quantities at the step n. First, $Q_{\text{MHD}}^{(n+1)}$ and $Q_{\text{PIC}}^{(n+1)}$ ($q_{\text{PIC}}^{(n+1)}$) are independently obtained by using Eq. (16). After that, we have $Q_{\text{interface}}^{(n+1)}$ according to the hand-shake scheme (13). In the PIC algorithm, particles in the interface domain are removed and new ones with microscopic quantities, $q_{\text{interface}}^{(n+1)}$, determined to satisfy $Q_{\text{interface}}^{(n+1)}$ are loaded. At the next step, we substitute $Q_{\text{interface}}^{(n+1)}$ and $q_{\text{interface}}^{(n+1)}$ in the right-hand side of Eq. (16) so as to obtain $Q_{\text{MHD}}^{(n+2)}$, $Q_{\text{PIC}}^{(n+2)}$, and $q_{\text{PIC}}^{(n+2)}$.

However, the electric field $\boldsymbol{E}$ and current density $\boldsymbol{J}$ are treated specifically, since they are not independent variables in the MHD algorithm, in which $\boldsymbol{E}_{\text{MHD}}$ and $\boldsymbol{J}_{\text{MHD}}$ are given as $\boldsymbol{E}_{\text{MHD}} = -\boldsymbol{u}_{\text{MHD}} \times \boldsymbol{B}_{\text{MHD}}$ and $\boldsymbol{J}_{\text{MHD}} = 1/(4\pi)\nabla \times \boldsymbol{B}_{\text{MHD}}$. By using Eq. (13), $\boldsymbol{E}_{\text{interface}}$ and $\boldsymbol{J}_{\text{interface}}$ are obtained; however, they are not used in Eq. (16) of the MHD algorithm, while they are substituted in the right-hand side of Eq. (16) of the PIC algorithm.

Furthermore, normalization constants of the MHD and PIC algorithms are different, hence, unit-transformation is required. For details, see Appendix B.

We show how time in our multi-hierarchy simulation advances in Fig. 3. A multi-time step scheme[12,14] is employed, where each of the MHD and PIC algorithms has different time steps. Large time steps are used for the MHD algorithm, and small ones are used for the PIC algorithm. For advancing the time from t_1 to t_2, the PIC algorithm receives interpolation values of MHD data at t_1 and at t_2 from the MHD algorithm at every PIC time step. On the other hand, at t_1, the MHD algorithm gets PIC data averaged over several steps around t_1.

The following procedure makes the simulation time advance from t_1 to t_2.

Step 1: Suppose that at t_1, physical quantities of the MHD and PIC algorithms are given.

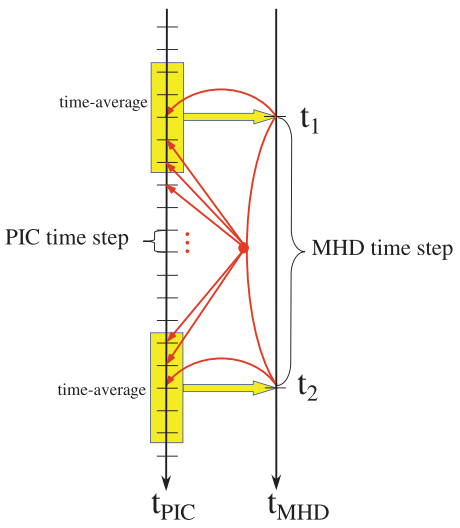

FIG. 3. Time-flow of the multi-hierarchy simulation. Large and small time steps are for MHD and PIC algorithms, respectively.

Step 2: The MHD algorithm sends MHD information at t_1 to the PIC algorithm.

Step 3: The PIC algorithm refers to MHD data at t_1 received in step 2 as Q_{MHD} in Eq. (13) and advances to $t_1 + \delta t$, where δt is a time period which corresponds to several time steps of the PIC algorithm.

Step 4: PIC information averaged over the period from $t_1 - \delta t$ to $t_1 + \delta t$ is sent to the MHD algorithm.

Step 5: The MHD algorithm advances one time step and reaches t_2, referring to PIC data obtained in step 4 as Q_{PIC} in Eq. (13).

Step 6: PIC information at $t_1 + \delta t$ which were obtained in step 3 is deleted and the PIC algorithm returns to t_1.

Step 7: The MHD algorithm sends MHD data at t_1 and those at t_2 to the PIC algorithm.

Step 8: During $t_1 < t < t_2$, the PIC algorithm refers to MHD data interpolated between at t_1 and at t_2 received in step 7 as Q_{MHD} in Eq. (13) and advances to t_2.

III. SIMULATION RESULTS

A. Examination: Plasma flow injection

In order to examine physical reliability of the interlocking method in the multi-hierarchy model with non-uniform space grids, we perform multi-hierarchy simulations of plasma injection from MHD to PIC domains. Figure 4 shows the schematic diagram of simulation box used in this subsection. The uniform magnetic field B_{x0} is taken to be the x direction (Simulation configuration is not suitable for magnetic reconnection.). The simulation domain is divided as follows: MHD domain: $48.0 < |y/(c/\omega_{ce})| < 106.75$, interface domain: $40.0 < |y/(c/\omega_{ce})| < 48.0$, and PIC domain: $|y/(c/\omega_{ce})| < 40.0$. The position y_c shown in Fig. 4 is taken to be $y_c/(c/\omega_{ce}) = 55.5$. The system is periodic in the x and z directions and is free in the y direction.

The simulation parameters are as follows. The ion-to-electron mass ratio is $m_i/m_e = 100$, and the ratio of the electron plasma frequency to the electron gyrofrequency is $\omega_{pe}/\omega_{ce} = 1.0$. The MHD time step is 0.1 in the MHD unit system and the PIC time step is 0.1 in the PIC unit system. According to the unit-transformation relation (B7) in Appendix B, MHD unit time is 10 times longer than PIC unit time. Thus, 10 PIC time steps correspond to 1 MHD time step. As the initial state, the mass density and magnetic field are uniform. The ion-electron temperature ratio is taken to be $T_{i0}/T_{e0} = 1.0$ at the initial time. The number of particles is 1 000 000 at the initial time and increases to $\simeq 1.59 \times 10^6$.

Plasma is supplied into the simulation box owing to $E \times B$ drift by imposing the driving electric field at the outside boundary of the MHD domain [$y/(c/\omega_{ce}) = \pm 106.75$]. The driving electric field, $E_{zd}(t)$, is programmed to evolve from zero to a constant value E_0 with a spatially uniform shape, where E_0 is $-0.06B_{x0}$ at $y/(c/\omega_{ce}) = -106.75$ and $0.06B_{x0}$ at $y/(c/\omega_{ce}) = 106.75$ in the PIC unit system. [In the MHD unit system, $|E_0|$ is $0.6B_{x0}$. See Eq. (B4) in Appendix B.]

Figure 5 shows the bird's eye view of the plasma mass density in the (y, x) plane at various times, where the mass density ρ is normalized to the initial uniform mass density ρ_0. We can see that low noise due to thermal fluctuations is excited in the PIC and interface domains. The plasma mass density in the MHD domain begins to increase at $\omega_{ce}t = 400$, and plasmas smoothly and continuously flow to the PIC domain via the interface domain. Consequently, plasmas pile up in the PIC domain and at $\omega_{ce}t = 1200$, two plasma flows have collided with each other at the center of the PIC domain.

This plasma injection process is a large-scale and slow phenomenon which can be treated within the MHD framework. Hence, we compare results of the multi-hierarchy simulation with those of pure MHD simulations, in which whole domain is calculated by the MHD algorithm. In Fig. 6, we display the spatial profiles of the mass density and magnetic field averaged in the x and z directions. Black and red lines represent results of the multi-hierarchy simulation and the pure MHD simulation, respectively. We can see that the mass density profiles (left panels) of the multi-hierarchy and

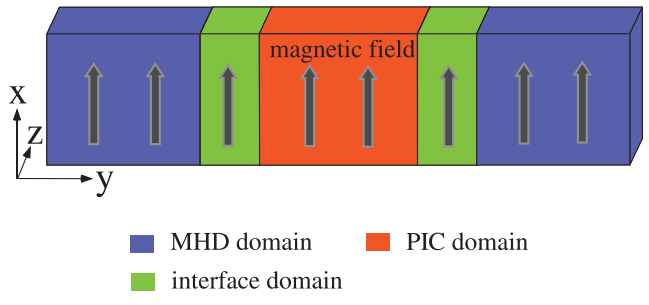

FIG. 4. Schematic diagram of the multi-hierarchy simulation box for examination of its validity, but not for magnetic reconnection.

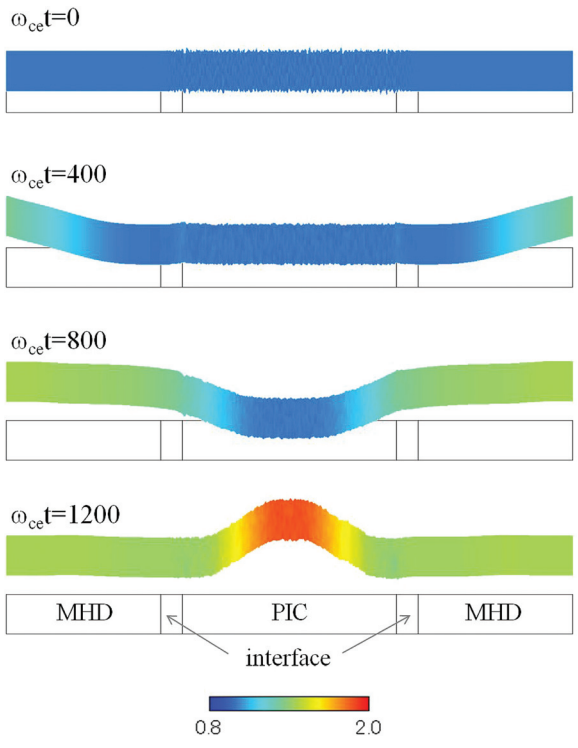

FIG. 5. Bird's eye view of the plasma mass density at $\omega_{ce}t = 0$, 400, 800, and 1200. Plasmas are injected inward and pile up in the PIC domain.

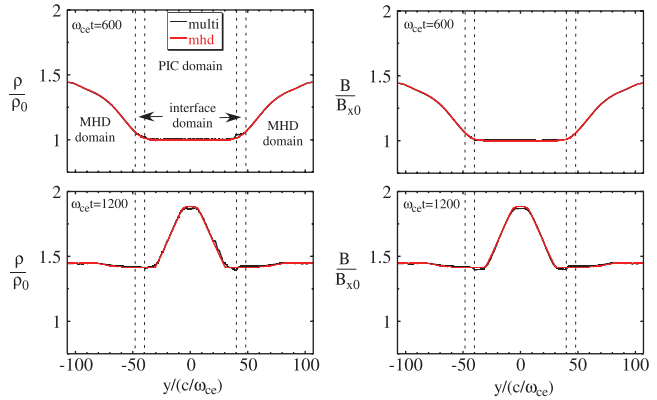

FIG. 6. Spatial profiles of mass density (left) and magnetic field (right) at $\omega_{ce}t = 600$ and 1200. Black and blue lines represent results of the multi-hierarchy and pure MHD simulations, respectively.

MHD simulations are almost the same, though, at $\omega_{ce}t = 600$, the profile of the multi-hierarchy simulation temporally has low noise in the interface domain. Also, the magnetic field profiles (right panels) of the multi-hierarchy simulations fit well to those from the MHD simulations.

These simulations demonstrate that at $\omega_{ce}t \simeq 1200$, the mass density and magnetic field profiles have formed a plateau structure, as shown in the bottom panels of Fig. 6 and have reached their maximum values in the vicinity of the center of the simulation domain ($y/(c/\omega_{ce}) \simeq 0$). So then, we observe the maximum values of the mass density $\rho_{\max}$ and the magnetic field $B_{x,\max}$ at $\omega_{ce}t = 1200$. In the multi-hierarchy simulation $\rho_{\max} = 1.88$ and $B_{x,\max} = 1.87$, while in the MHD simulation $\rho_{\max} = 1.87$ and $B_{x,\max} = 1.89$. Both maximum values of the mass density and magnetic field from the multi-hierarchy simulations are in good agreement with those from the MHD simulations. It is confirmed that the interlocking method in the multi-hierarchy model with the non-uniform space grids describes the physics correctly in the same way as that with the uniform space grids, as shown in Ref. 14.

B. Collisionless driven reconnection

Next, we apply our multi-hierarchy simulation model to collisionless magnetic reconnection in an open system.[19] Here, the simulation box is shown in Fig. 1. The simulation domain is implemented on a $(256 \times 303 \times 4)$ point grid and a box size is $64(c/\omega_{ce}) \times 114.75(c/\omega_{ce}) \times 1.0(c/\omega_{ce})$. The simulation domain is divided as follows: MHD domain: $19.875 < |y/(c/\omega_{ce})| < 57.375$, interface domain: $17.875 < |y/(c/\omega_{ce})| < 19.875$, and PIC domain: $|y/(c/\omega_{ce})| < 17.875$. The position y_c shown in Fig. 2 is taken to be $|y_c/(c/\omega_{ce})| = 24.75$. The system is periodic in the z direction and is free in the x and y directions.

The simulation parameters are as follows. The ion-to-electron mass ratio is $m_i/m_e = 100$, and the ratio of the electron plasma frequency to the electron gyrofrequency is $\omega_{pe}/\omega_{ce} = 1.5$. The MHD time step is 0.05 in the MHD unit system and the PIC time step is 0.05 in the PIC unit system. Referring to the unit-transformation equation (B7) in Appendix B, MHD unit time is equal to 15 times PIC unit time. Thus, 15 PIC time steps correspond to 1 MHD time step. The initial condition is given by a one-dimensional Harris-type equilibrium as $B_x(y) = B_0 \tanh(y/L_y)$ for the magnetic field and $n_p(y) = n_{p0}/\cosh^2(y/L_y)$ for the number density, where B_0 and n_{p0} are constant and L_y is the spatial scale. The ion-electron temperature ratio is taken to be $T_{i0}/T_{e0} = 1.0$. The number of particles contributing to n_p is 2 000 000 at the initial time. In addition to the so-called foreground plasmas n_p, the non-uniform background plasmas[19,20] expressed as $n_b(y) = n_{b0}[1 - 1/\cosh^2(y/L_y)]$ also exist, where n_{b0} has a constant value $n_{b0}/n_{p0} = 0.25$. Although this background plasmas give rise to a weak pressure imbalance, according to Refs. 19 and 20, it is quickly justified without

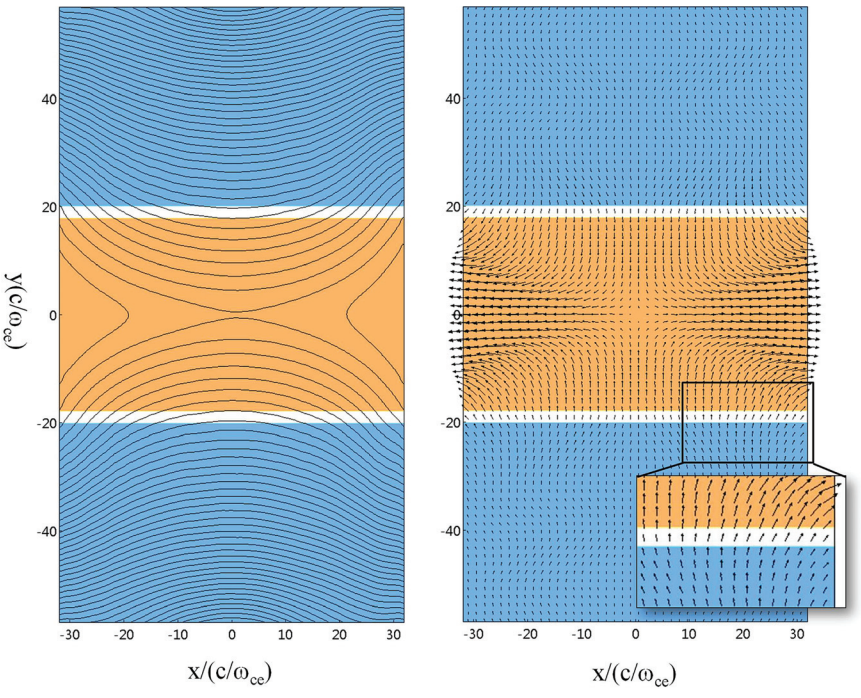

FIG. 7. Spatial profiles of magnetic field lines (left) and vector plots of fluid velocity (right) in the (x, y) plane at $\omega_{ce}t = 2430$. Light blue, light brown, and white areas show the MHD, PIC, and interface domains, respectively.

any significant modification of the current sheet structure. The total number of particles thus is $\simeq 2.45 \times 10^6$ at the initial time and increases to $\simeq 3.82 \times 10^6$.

The driving electric field, $E_{zd}(x,t)$, imposed at the upstream boundary of the MHD domain $[y/(c/\omega_{ce}) = \pm 57.375]$ is programmed to evolve from zero to a constant value, $E_0 = -0.04B_{x0}$, in the PIC unit system. [$E_0 = -0.6B_{x0}$ in the MHD unit system. See Eq. (B4) in Appendix B.] The field $E_{zd}(x,t)$ is set to zero at the initial time and begins to grow at $x = 0$. The width of the region where $E_{zd}(x,t)$ grows is gradually increased. Eventually, $E_{zd}(x,t)$ develops to reach E_0 on the entire boundary of the MHD domain.

Figure 7 demonstrates the spatial profiles of magnetic field line (left panel) and vector plots of the fluid velocity (right panel) in the (x,y) plane at $\omega_{ce}t = 2430$. An enlarged view of vector plots in the rectangular region, which covers the interface domain near the downstream boundary, is also presented. Clearly, both plasma and magnetic flux are smoothly supplied to the PIC domain (light brown area) through the interface domain (white area) from the MHD domain (light blue area), and the reconnected flux moves out smoothly from the downstream region.

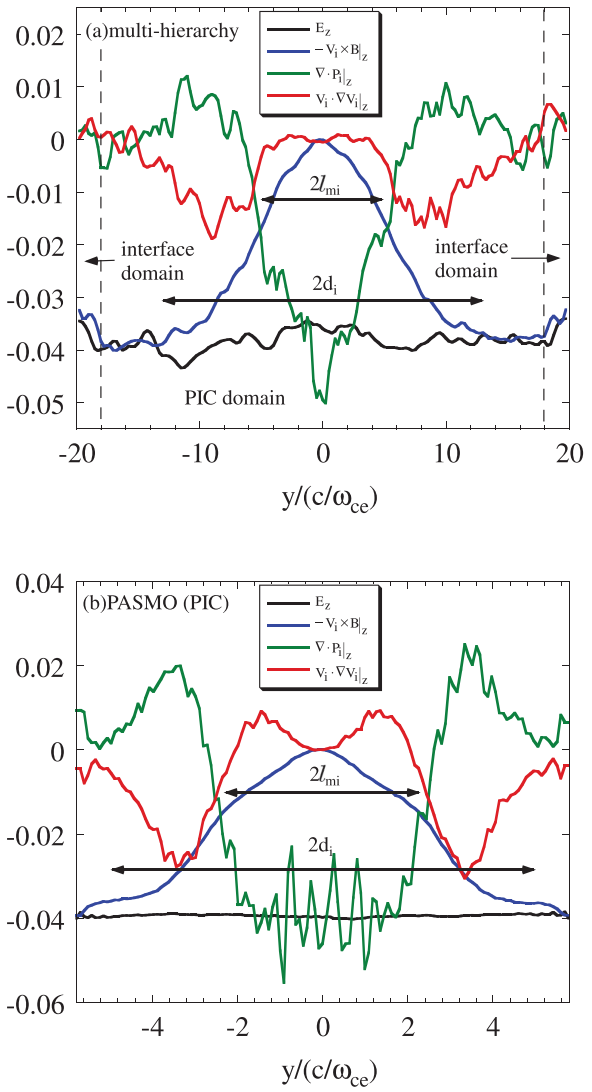

FIG. 8. Spatial profiles of various terms in the z-component of the ion force balance equation along y axis. (a) Multi-hierarchy simulation, (b) PASMO (PIC) simulation.

Next, let us compare the multi-hierarchy simulation results with those from the PIC simulation code named PASMO, in order to get the physical verification of magnetic reconnection found in our multi-hierarchy model. The PASMO is a three-dimensional electromagnetic PArticle Simulation code for investigating driven Magnetic reconnection in an Open system, which has been developed and progressed by Horiuchi, Ohtani *et al.*[7,8,19] Figure 8(a) shows the spatial profiles of the non-ideal terms in the z-component of the ion force balance equation at $\omega_{ce}t = 2430$, which is obtained by the multi-hierarchy simulation. The pressure tensor term (green line) becomes dominant within the ion meandering scale $l_{mi} \simeq 4.9(c/\omega_{ce})$ and it mainly sustains the reconnection electric field (black line) in the central current layer. The inertia term (red line) grows in the intermediate region of $l_{mi} < |y| < d_i \simeq 13.0(c/\omega_{ce})$, where d_i is the ion inertial length, but it is almost canceled out by the pressure tensor term with the opposite sign. Meanwhile, in Fig. 8(b), we display the profiles from the PASMO simulation for $m_i/m_e = 50$ and $\omega_{pe}/\omega_{ce} = 2.5$ at $\omega_{ce}t = 1023$. The results from the multi-hierarchy simulation are consistent with those from the PASMO simulations. Thus, our present multi-hierarchy model with non-uniform spatial grids can describe collisionless driven reconnection in an open system as a multi-hierarchy phenomenon with the high accuracy.

IV. SUMMARY

We have extended our previous multi-hierarchy simulation model[12–16] for the analysis of magnetic reconnection to the more realistic model with non-uniform space grids. This model consists of three parts: an MHD algorithm with a large time step and non-uniform space grids to describe the global dynamics away from the reconnection point, a PIC algorithm with fine-grained space grids to express the microscopic kinetic process near the reconnection point, and an interface algorithm to treat interconnection between the macro hierarchy (MHD algorithm) and the micro hierarchy (PIC algorithm).

For examining physical reliability of the interlocking method, we have performed simulations of plasma flow injection into a system with uniform profiles by using our improved multi-hierarchy model. Plasmas are injected smoothly and continuously from the MHD to the PIC domains through the interface domain. It is observed that profiles of the plasma mass density and magnetic field in the multi-hierarchy simulation are almost the same as those from the pure MHD simulations.

We have further applied this model to collisionless magnetic reconnection in an open system. We can see that plasma inflows come inward from the MHD domain and drive magnetic reconnection in the PIC domain. Furthermore, the physical validity of magnetic reconnection found in the multi-hierarchy simulation is confirmed by comparing the simulation results with the PASMO simulation results.

Several problems remain unsolved for full understanding of magnetic reconnection as a multi-hierarchy phenomenon. One problem is how to construct an interlocking algorithm in the downstream direction. Fast plasma outburst towards the downstream direction is generated as a result of magnetic reconnection, and makes the particle velocity distribution far from Maxwellian.[21,22] Some kinds of relaxation processes are required to interlock the PIC domain with the MHD domain. The other problem is the method for generating a kinetic region (micro hierarchy) in a dynamically evolving macroscopic system. An appropriate interlocking method can reduce the computer resources and enable our multi-hierarchy simulation model to be applicable to magnetic reconnection in more realistic systems in near future.

ACKNOWLEDGMENTS

This simulation work was performed by employing the Plasma Simulator at the National Institute for Fusion Science. This work was partially supported by a Grant-in-Aid for Scientific Research from the Japan Society for the Promotion of Science (Grant Nos. 23340182 and 24740374), the Research Cooperation Program on Hierarchy and Holism in Natural Sciences at the National Institutes of Natural Sciences, and the General Coordinated Research at the National Institute for Fusion Science (NIFS11KNTS009 and NIFS11KNSS018).

APPENDIX A: INTERCONNECTION FUNCTION FOR PRESSURE

As the interconnection function F, Eq. (15) is used only for pressure (thermal velocities). The reason derives from how to treat microscopic quantities in the interface domain. When the PIC algorithm calculates a thermal velocity by assembling particle velocities statistically, the obtained value contains a numerical error $v_T(1+\delta)$, where v_T is the exact thermal velocity and δ is a numerical error factor. In general, an averaged numerical error $\langle\delta\rangle$ is not zero.

As discussed in Sec. III B, all particles in the interface domain are removed and new particles satisfying macroscopic quantities such as the new thermal velocities are loaded at every PIC time step. In other words, the process that the PIC algorithm calculates a thermal velocity by assembling these particle velocities statistically, generates a Maxwellian distribution with a thermal velocity calculated, and again calculates a thermal velocity is repeated. At first, the exact thermal velocity is v_T, however, $v_T(1+\delta)$ is measured. As a result, particles with a thermal velocity $v_T(1+\delta)$ are loaded. Next, the PIC algorithm assembles these particle velocities statistically again, and measure $v_T(1+\delta)^2$ as a thermal velocity if Eq. (14) is employed as F. The error δ would be quite small. However, this process is operated many times, thus, the error would grow exponentially to give rise to unphysical heating or cooling.[23]

APPENDIX B: OVERVIEW OF UNIT-TRANSFORMATION

In order to exchange physical quantities between the MHD and PIC algorithms in the interface domain, the unit-transformation is needed, since normalization constants are completely different from each other. Table I represents physical quantities and their normalization constants in the MHD and PIC algorithms. For instance, velocities in the MHD algorithm are normalized to the Alfvén speed v_A, while ones in the PIC algorithm are normalized to the speed of light c.

We show the unit-transformation of physical quantities calculated by the PIC algorithm. We need to determine two following relations:

$$B_n = \frac{m_e^{\mathrm{SP}} c\omega_{ce}}{q_e^{\mathrm{SP}}}, \tag{B1}$$

$$L = \alpha(c/\omega_{ce}), \tag{B2}$$

where B_n is the normalization constant of a magnetic field in the MHD algorithm and is arbitrary, m_e^{SP} is the electron super-particle mass, ω_{ce} is the electron gyrofrequency, q_e^{SP} is the electron super-particle charge, and L is arbitrary length. The parameter α can be determined freely. In this paper, α is taken to be 1.0 for all simulations. They mean that normalization constant of magnetic field in the MHD algorithm equals that of the PIC algorithm and the MHD unit length is α times the PIC unit length. Furthermore, in particle simulations, the ion-to-electron mass ratio m_i/m_e and the ratio of the electron plasma frequency to the electron gyrofrequency ω_{pe}/ω_{ce} which is satisfied at the standard electron number density n_{e0} are given as certain values. For instance, in Sec. III A, $m_i/m_e = 100$ and $\omega_{pe}/\omega_{ce} = 1.0$ at $n_{e0,\mathrm{P}} = 2604.2$ are employed. Therefore, we can transform PIC quantities in the PIC unit system to those in the MHD unit system as follows:

$$\boldsymbol{B}_{\mathrm{M}} = \boldsymbol{B}_{\mathrm{P}}, \tag{B3}$$

$$\boldsymbol{E}_{\mathrm{M}} = \frac{\omega_{pe}}{\omega_{ce}}\sqrt{\frac{m_i}{m_e}}\boldsymbol{E}_{\mathrm{P}}, \tag{B4}$$

$$r_{\mathrm{M}} = \frac{1}{\alpha} r_{\mathrm{P}}, \tag{B5}$$

TABLE I. Normalization constants in the MHD and PIC governing equations. Here, L, B_n, and ρ_n are arbitrary length, magnetic field, and mass density, respectively, c is the speed of light, ω_{ce} is the electron gyrofrequency, v_A is the Alfvén speed defined as $v_A = B_n(4\pi\rho_n)^{-1/2}$, m_e^{SP} is the electron super-particle mass, and q_e^{SP} is the electron super-particle charge.

	Normalization constant	
Quantity	MHD	PIC
Length	L	c/ω_{ce}
Velocity	v_A	$\boldsymbol{c}$
Time	L/v_A	$1/\omega_{ce}$
Magnetic field	B_n	$m_e^{\mathrm{SP}} c\omega_{ce}/q_e^{\mathrm{SP}}$
Electric field	$v_A B_n$	$m_e^{\mathrm{SP}} c\omega_{ce}/q_e^{\mathrm{SP}}$
Mass	…	m_e^{SP}
Charge	…	q_e^{SP}
Number density	…	$(c/\omega_{ce})^{-3}$
Mass density	ρ_n	$m_e^{\mathrm{SP}}(c/\omega_{ce})^{-3}$
Pressure	$\rho_n v_A^2$	$m_e^{\mathrm{SP}} c^2(c/\omega_{ce})^{-3}$
Current density	$B_n/(4\pi L)$	$q_e^{\mathrm{SP}} c(c/\omega_{ce})^{-3}$

$$\boldsymbol{u}_{\mathrm{M}} = \frac{\omega_{pe}}{\omega_{ce}}\sqrt{\frac{m_i}{m_e}}\boldsymbol{u}_{\mathrm{P}} = \frac{\omega_{pe}}{\omega_{ce}}\sqrt{\frac{m_i}{m_e}}\frac{\boldsymbol{u}_{e,\mathrm{P}} + (m_i/m_e)\boldsymbol{u}_{i,\mathrm{P}}}{1+(m_i/m_e)}, \quad \text{(B6)}$$

$$t_{\mathrm{M}} = \frac{1}{\alpha}\frac{\omega_{ce}}{\omega_{pe}}\sqrt{\frac{m_e}{m_i}}t_{\mathrm{P}}, \quad \text{(B7)}$$

$$\rho_{\mathrm{M}} = \frac{1}{n_{e0,\mathrm{P}}}\left(\frac{m_e}{m_i}\right)\rho_{\mathrm{P}} = \frac{1}{n_{e0,\mathrm{P}}}\left[n_{e,\mathrm{P}}\left(\frac{m_e}{m_i}\right) + n_{i,\mathrm{P}}\right], \quad \text{(B8)}$$

$$P_{\mathrm{M}} = \left(\frac{\omega_{pe}}{\omega_{ce}}\right)^2\frac{1}{n_{e0,\mathrm{P}}}P_{\mathrm{P}} = \left(\frac{\omega_{pe}}{\omega_{ce}}\right)^2\frac{1}{n_{e0,\mathrm{P}}}\left[n_{e,\mathrm{P}}v_{Te,\mathrm{P}}^2 + n_{i,\mathrm{P}}v_{Ti,\mathrm{P}}^2\left(\frac{m_i}{m_e}\right)\right], \quad \text{(B9)}$$

$$\boldsymbol{J}_{\mathrm{M}} = \alpha\left(\frac{\omega_{pe}}{\omega_{ce}}\right)^2\frac{1}{n_{e0,\mathrm{P}}}\boldsymbol{J}_{\mathrm{P}} = \alpha\left(\frac{\omega_{pe}}{\omega_{ce}}\right)^2\frac{n_{i,\mathrm{P}}\boldsymbol{u}_{i,\mathrm{P}} - n_{e,\mathrm{P}}\boldsymbol{u}_{e,\mathrm{P}}}{n_{e0,\mathrm{P}}}, \quad \text{(B10)}$$

where r, $\boldsymbol{u}$, $\boldsymbol{u}_e$, $\boldsymbol{u}_i$, t, v_{Te}, and v_{Ti} denote the length, one-fluid velocity, electron fluid velocity, ion fluid velocity, time, electron thermal velocity, and ion thermal velocity, respectively, and the subscripts M and P mean quantities normalized in the MHD and PIC unit systems, respectively. Also, we would like to describe that in the MHD equations, the electric field is defined not as $\boldsymbol{E} = -(\boldsymbol{u}/c)\times\boldsymbol{B}$ which is given from the generalized Ohm's law, but as $\boldsymbol{E} = -\boldsymbol{u}\times\boldsymbol{B}$. Thereby, the normalization constant of the electric field is different from that of the magnetic field in the MHD equations, while the normalization constants of the electric and magnetic fields are the same in the PIC equations. That leads to a factor between $\boldsymbol{E}_{\mathrm{M}}$ and $\boldsymbol{E}_{\mathrm{P}}$ in Eq. (B4).[24]

Let us note that quantities on the left-hand side of Eqs. (B3)–(B10) are measured in the MHD unit system, however, they are not data computed by the MHD algorithm, but simulated by the PIC algorithm. In other words, quantities such as $\boldsymbol{B}_{\mathrm{M}}$ and ρ_{M} correspond to Q_{PIC} in Eq. (13). Transforming from the PIC to the MHD unit systems as shown in Eqs. (B3)–(B10), we operate the hand-shake scheme (13) in order to give macroscopic physical quantities in the interface domain.

On the other hand, solving physics in the interface domain with the PIC algorithm requires transformation of $Q_{\mathrm{interface}}$ in the MHD unit system into $Q_{\mathrm{interface}}$ in the PIC unit system. Furthermore, in order to produce Maxwellian velocity distribution, fluid (averaged) velocities, thermal velocities, and number densities of electrons and ions in the PIC unit system are needed. Therefore, assuming that electrons and ions have the same number density[25] and temperature, we transform the fluid velocity, mass density and pressure in the MHD unit system to the number densities, fluid (averaged) velocities, and thermal velocities of electrons and ions in the PIC unit system, respectively, as follows:

$$n_{e,\mathrm{P}} = n_{i,\mathrm{P}} = \frac{1}{(m_e/m_i)+1}n_{e0,\mathrm{P}}\rho_{\mathrm{M}}, \quad \text{(B11)}$$

$$\boldsymbol{u}_{e,\mathrm{P}} = \frac{\omega_{ce}}{\omega_{pe}}\sqrt{\frac{m_e}{m_i}}\boldsymbol{u}_{\mathrm{M}} - \frac{1}{\alpha}\left(\frac{\omega_{ce}}{\omega_{pe}}\right)^2\left(\frac{m_e}{m_i}+1\right)\frac{\boldsymbol{J}_{\mathrm{M}}}{\rho_{\mathrm{M}}}, \quad \text{(B12)}$$

$$\boldsymbol{u}_{i,\mathrm{P}} = \frac{\omega_{ce}}{\omega_{pe}}\sqrt{\frac{m_e}{m_i}}\boldsymbol{u}_{\mathrm{M}}, \quad \text{(B13)}$$

$$v_{Te,\mathrm{P}}^2 = \frac{1}{2}\left(\frac{\omega_{ce}}{\omega_{pe}}\right)^2\left(\frac{m_e}{m_i}+1\right)\frac{P_{\mathrm{M}}}{\rho_{\mathrm{M}}}, \quad \text{(B14)}$$

$$v_{Ti,\mathrm{P}}^2 = \frac{1}{2}\left(\frac{\omega_{ce}}{\omega_{pe}}\right)^2\left(\frac{m_e}{m_i}+1\right)\left(\frac{m_e}{m_i}\right)\frac{P_{\mathrm{M}}}{\rho_{\mathrm{M}}}. \quad \text{(B15)}$$

The electron fluid velocity is determined by Eq. (B12), since the difference between ion and electron fluid velocities expresses an electric current in the PIC algorithm.

[1]N. A. Krall and P. C. Liewer, Phys. Rev. **4**, 2094 (1971).
[2]W. Daughton, G. Lapenta, and P. Ricci, Phys. Rev. Lett. **93**, 105004 (2004).
[3]R. Horiuchi and T. Sato, Phys. Plasmas **6**, 4565 (1999).
[4]T. Moritaka and R. Horiuchi, Phys. Plasmas **15**, 092114 (2008).
[5]R. Horiuchi and T. Sato, Phys. Fluids B **1**, 581 (1989).
[6]M. M. Kuznetosova, M. Hesse, L. Rastätter, A. Taktakishvili, G. Toth, D. L. Zeeuw, A. Ridley, and T. I. Gombosi, J. Geophys. Res. **112**, A10210, doi:10.1029/2007JA012316 (2007).
[7]W. Pei, R. Horiuchi, and T. Sato, Phys. Plasmas **8**, 3251 (2001).
[8]W. Pei, R. Horiuchi, and T. Sato, Phys. Rev. Lett. **87**, 235003 (2001).
[9]A. Ishizawa and R. Horiuchi, Phys. Rev. Lett. **95**, 045003 (2005).
[10]R. Horiuchi and T. Sato, Phys. Plasmas **4**, 277 (1997).
[11]B. Li and R. Horiuchi, Phys. Rev. Lett. **101**, 215001 (2008).
[12]S. Usami, H. Ohtani, R. Horiuchi, and M. Den, Comm. Comput. Phys. **4**, 537 (2008).
[13]R. Horiuchi, S. Usami, H. Ohtani, and M. Den, J. Plasma Fusion Res. **8**, 184 (2009).
[14]S. Usami, H. Ohtani, R. Horiuchi, and M. Den, Comm. Comput. Phys. **11**, 1006 (2012).
[15]S. Usami, H. Ohtani, R. Horiuchi, and M. Den, J. Plasma Fusion Res. **4**, 049 (2009).
[16]R. Horiuchi, S. Usami, H. Ohtani, and T. Moritaka, J. Plasma Fusion Res. **5**, S2006 (2010).
[17]C. K. Birdsall and A. B. Langdon, *Plasma Physics via Computer Simulation* (McGraw-Hill, New York, 1985).
[18]T. Sugiyama and K. Kusano, J. Comput. Phys. **227**, 1340 (2007).
[19]H. Ohtani and R. Horiuchi, J. Plasma Fusion Res. **4**, 024 (2009).
[20]I. Shinohara, H. Suzuki, M. Fujimoto, and M. Hoshino, Phys. Rev. Lett. **87**, 095001 (2001).
[21]R. Horiuchi and H. Ohtani, Comm. Comput. Phys. **4**, 496 (2008).
[22]M. Hesse, Phys. Plasmas **13**, 122107 (2006).

[23]Unphysical heating or cooling would occur in the case that the program code generating (shifted) Maxwellian distribution has the similar tendency, too.
[24]The same is equally true of the current density. In the MHD equations, we define the current density not as $\boldsymbol{J} = c/(4\pi)\nabla\times\boldsymbol{B}$ which is derived from the Ampere's law, but as $\boldsymbol{J} = 1/(4\pi)\nabla\times\boldsymbol{B}$. That however does not cause a complicated factor in Eq. (B10).
[25]In PIC simulations, a slight local difference in charge density between ions and electrons, $\delta n = n_i - n_e$, is often generated. In order to conserve the charge neutrality in the entire system, the following procedure is done. The ion number density $n_{i,\mathrm{P}}$ is given by the relation (B11) with no change. While for the electron number density, Eq. (B11) is modified to $n_{e,\mathrm{P}} = ([m_e/m_i]+1)^{-1}n_{e0,\mathrm{P}}\rho_{\mathrm{M}} - \delta n$. Here δn is required to be much less than n_i, otherwise such a region cannot be interlocked to the MHD algorithm.